Neutral Sulfur Atom Formation in Decay of Deep Core Holes in SF_6

Oksana Travnikova,[1,*] Florian Trinter,[2,3,†] Marcus Agåker,[4,5] Giorgio Visentin,[6,7] Joakim Andersson,[8] Ludvig Kjellsson,[4] Iyas Ismail,[1] Nicolas Velasquez,[1] Dimitris Koulentianos,[1] Manuel Harder,[9] Zhong Yin,[10] Johan Söderström,[4] Tatiana Marchenko,[1] Renaud Guillemin,[1] O. Dennis McGinnis,[3] Hans Ågren,[4] Stephan Fritzsche,[6,7,11] Marc Simon,[1] Jan-Erik Rubensson,[4] and Joseph Nordgren[4,‡]

[1]*Sorbonne Université, CNRS, UMR 7614, Laboratoire de Chimie Physique-Matière et Rayonnement, F-75005 Paris, France*
[2]*Molecular Physics, Fritz-Haber-Institut der Max-Planck-Gesellschaft, Faradayweg 4-6, 14195 Berlin, Germany*
[3]*Institut für Kernphysik, Goethe-Universität Frankfurt, Max-von-Laue-Straße 1, 60438 Frankfurt am Main, Germany*
[4]*Department of Physics and Astronomy, Uppsala Universitet, Box 516, 751 20 Uppsala, Sweden*
[5]*MAX IV Laboratory, Lund University, PO Box 118, SE-22100 Lund, Sweden*
[6]*GSI Helmholtzzentrum für Schwerionenforschung, Planckstraße 1, 64291 Darmstadt, Germany*
[7]*Helmholtz-Institut Jena, Fröbelstieg 3, 07743 Jena, Germany*
[8]*Division of Solid State Electronics, Department of Electrical Engineering, Uppsala University, Box 65, SE-751 03 Uppsala, Sweden*
[9]*European XFEL, Holzkoppel 4, 22869 Schenefeld, Germany*
[10]*International Center for Synchrotron Radiation Innovation Smart, Tohoku University, Sendai 980-8572, Japan*
[11]*Theoretisch-Physikalisches Institut, Friedrich-Schiller-Universität Jena, Max-Wien-Platz 1, 07743 Jena, Germany*

(Received 20 July 2024; accepted 10 January 2025; published 12 February 2025)

Dissociation upon sulfur K-shell excitation or ionization of SF_6 is studied by sulfur L-shell emission spectroscopy using synchrotron radiation and multiconfiguration Dirac-Hartree-Fock calculations of emission energies and transition rates. The decay path involves in particular Auger emission with the ejection of one or more electrons, leading to singly or multiply charged intermediate states. Nevertheless, the results of the study show that the observed photon emission at 151–152 eV following excitation at 2485–2489 eV originates dominantly from transitions in neutral sulfur. This clearly indicates that the central atom retains its electrons in a dissociation process where all fluorine atoms detach before the S $2p$ decay.

DOI: 10.1103/PhysRevLett.134.063003

The interaction of x-rays with matter typically results in a complex interplay of absorption, scattering, ionization, decay of excited states, and nuclear rearrangement. Apart from the fundamental interest in these intricate processes, understanding the effects of x-ray irradiation is crucial for the advancement in numerous scientific and engineering disciplines. Moreover, the interactions are important for applications ranging from medical imaging and therapy to manipulation of materials.

Tender and hard x-rays create deep electron vacancies that are characterized by very short lifetimes on the order of 1 fs or less [1]. The decay pathways involved proceed through a series of sequential relaxation steps, including Auger (also sometimes called Auger-Meitner) decay and x-ray emission. Numerous fragments are typically observed in the various steps of the Auger cascades, primarily due to Coulomb repulsion. In some cases, dissociation occurs on the same timescale as the core-hole decay, e.g., following Cl $1s \rightarrow \sigma^*$ excitation in HCl [2]. This is a consequence of the formation of strongly dissociative and/or multiply charged core-hole intermediate states, which subsequently undergo fragmentation through processes known as ultrafast dissociation (UFD) and Coulomb explosion. The dissociation process that occurs during multistep cascade decays is termed MUST UFD (multistep ultrafast dissociation) to distinguish it from UFD processes associated with the single-step relaxation of shallow core-hole intermediates [2].

UFD studies employing resonant Auger electron spectroscopy and resonant inelastic x-ray scattering (RIXS) represent a powerful and comprehensive approach to elucidate the complex dynamics of molecular systems on ultrafast timescales [3–7]. In particular, x-ray emission may offer a higher degree of resolution and contrast in some cases as it is not affected by charge distribution, unlike Auger electron emission.

In an early high-resolution study of sulfur L x-ray emission of SF_6, excited by 10 keV electron impact, a distinct group of very narrow lines at 151–152 eV was

*Contact author: oksana.travnikova@upmc.fr
†Contact author: trinter@fhi-berlin.mpg.de
‡Contact author: joseph.nordgren@physics.uu.se

observed, indicating complete detachment of the fluorine atoms [8]. The emission clearly showed that S $2p$ core-hole states with sufficient lifetime to allow dissociation prior to decay were formed [9,10]. In the hard x-ray regime, dissociation can occur during the subsequent decay steps of the relaxation cascade, except for the first step, which is usually characterized by an extremely short lifetime with very little freedom for nuclear dynamics.

In the present work, we used monochromatized synchrotron radiation to selectively study the L emission from S $1s$ excited SF_6 in the gas phase. This selectivity enables us to clearly separate the resonant S $1s$ excitation in the neutral molecule from ionization, with the direct S $2p$ excitation channel excluded in both cases, unlike the previous experiment. To reveal the underlying decay dynamics, detailed calculations have been performed on the transition energies and decay rates of the different steps of the decay to investigate the origin of the observed lines. The study shows that although single or multiple ionization takes place in the early phase of the decay path, due to Auger relaxation, the final x-ray emission step takes place in predominantly neutral sulfur atoms.

The experiments were carried out at beamline P04 of the PETRA III synchrotron facility in Hamburg, which offers circularly polarized x-rays in the 250–3000 eV range with fluxes up to several 10^{12} photons per second and a resolving power of over 10^4 [11].

The spectrometer used was a compact Grace-type grazing-incidence Rowland instrument that has been used in numerous experiments since its conception in 1987 [12]. Its acceptance angle was $\sim 3 \times 10^{-4}$ steradians, employing a 1200 mm^{-1} grating and no entrance slit. The detector was a CsI-coated microchannel plate (MCP) sensor with phosphor-screen display. While the size of the source determined the resolution of the outgoing photons, this was not limited by the spatial resolution of the MCP detector. Instead, the limiting factor was the smallest exit slit of the monochromator compatible with adequate signal strength, resulting in a resolution of 0.25 eV.

A constant flow of SF_6 gas through a gas cell, separated from vacuum by a 150 nm diamondlike carbon membrane [13], was maintained. This allowed us to replenish the sample and to avoid interference signals from fragments. The gas-cell arrangement was similar to previous molecular RIXS studies [3], though special attention was required to optimize signal due to the longer absorption length of the 2.5 keV exciting photons in SF_6 compared to the 150 eV emitted photons. Figure 1 shows the experimental setup at beamline P04 at PETRA III with the Grace spectrometer and the gas-cell arrangement.

A grazing angle of incidence was used to achieve maximum absorption of the exciting radiation and minimize self-absorption of emitted radiation. Transmission of both exciting and emitted radiation through the membrane and the sample gas are the primary factors that control the

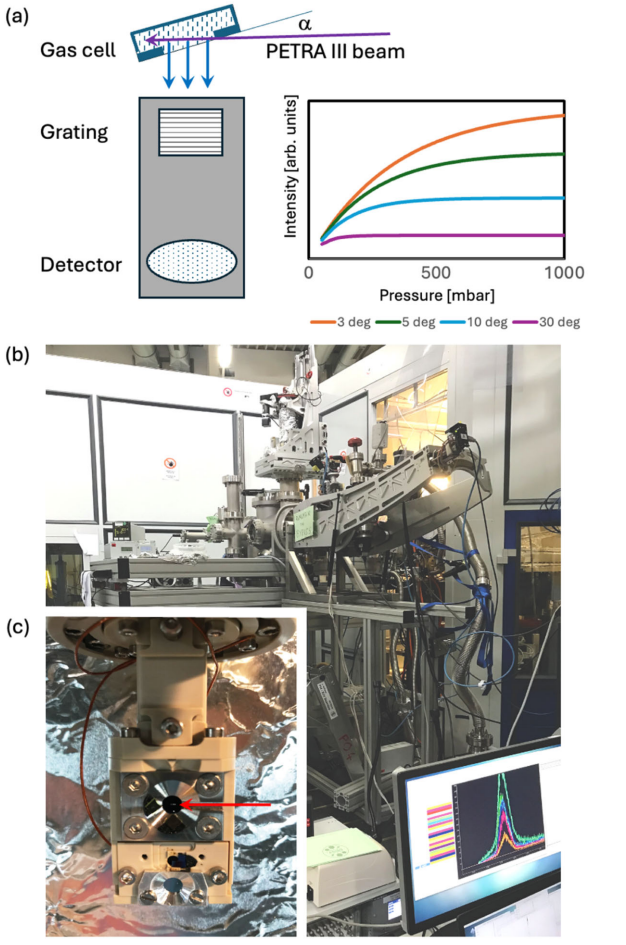

FIG. 1. (a) Experimental setup at PETRA III and graph showing the dependence of L-emission intensity on SF_6 gas pressure for different incidence angles. (b) Photo of the spectrometer setup. The PETRA III beam enters from the right. (c) Inset showing details of the gas cell. Arrow shows how the beam enters onto the carbon membrane.

intensity dependence on the angle of incidence. In practice, only a limited range of sample gas pressures can be accessed if the angle of incidence is not sufficiently small. A compromise pressure of ~300–400 mbar was chosen to optimize signal and membrane lifetime, see Fig. 1. The dissociation products of SF_6 severely etched the membrane, necessitating replacement approximately every 7 h.

The sulfur L emission from gaseous SF_6 was measured at different photon energies, from 2450 to 2500 eV, i.e., in steps from well below the $1s \rightarrow 6t_{1u}$ resonance to above the ionization threshold. The resulting spectra are shown in Fig. 2, in the lowermost part, as color-coded composite spectra recorded at different excitation energies. This exhibits an excitation-energy-dependent spectral feature centered at 151.5 eV photon energy. In the middle part of the figure peak-normalized spectra are shown. In addition to the strongly resonant structure, there are features at photon energies corresponding to the molecular

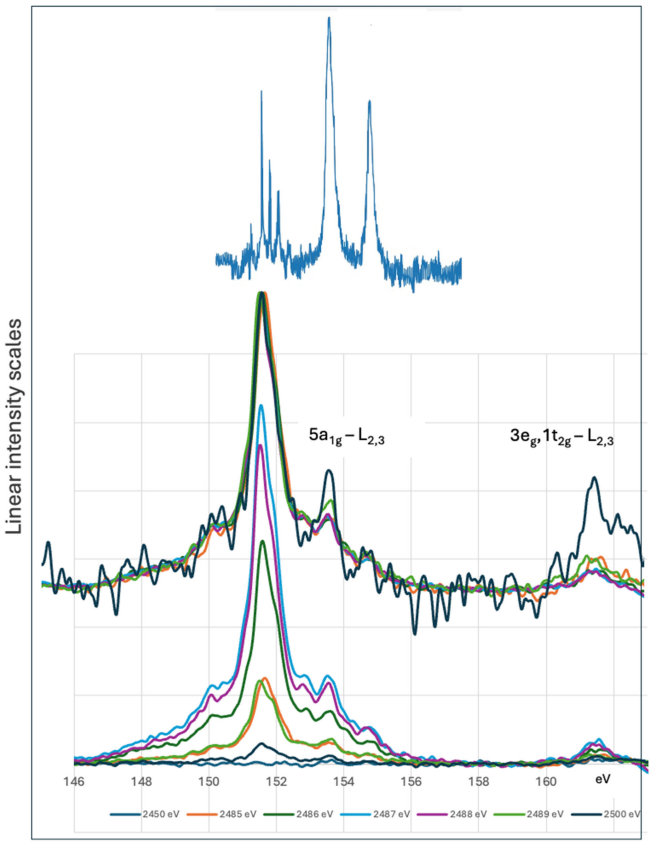

FIG. 2. L-emission spectra of gaseous SF_6. Lowermost spectra excited at various photon energies below and near the S $1s \rightarrow 6t_{1u}$ resonance energy 2487 eV, as well as above the ionization threshold. Middle spectra are peak normalized. Uppermost spectrum is excited by 10 keV electrons [8].

$5a_{1g} - 2p_{1/2,3/2}$ and $3e_g$, $1t_{2g} - 2p_{1/2,3/2}$ transitions [8], i.e., in the not dissociated molecule. The relative intensities of these emission lines increase with the excitation energy and especially above the ionization threshold, supporting identifying these features as molecular emission lines. The uppermost spectrum in the figure is an excerpt from the original study mentioned above [8]. The resolution in the present experiment is not sufficient to clearly resolve the components apparently present in this spectral feature. A closer look at the structure reveals some excitation-dependent variations in the relative intensities between the components. This, together with the observation in Ref. [8], suggests a dependence of the population of atomic states responsible for photon emission on the excitation energy. In the Supplemental Material [14], this dependence is presented in more detail.

Given the observations of the 151–152 eV lines at 10 keV electron-beam excitation, the analysis strategy begins with calculations of atomic sulfur emission associated with atomic S $2p$ hole states. The quite limited energy range of the observed spectrum and the high accuracy of the calculations ($\leqslant$1 eV) offers a means to identify the specific transitions with the aim to identify specific states populated in the dissociative decay path following S $1s$ excitation. Furthermore, there are experimental indications of S $2p$ hole states being dissociative. In a study of gaseous carbonyl sulfide using Auger and x-ray emission, one observes dissociation upon L_2 and L_3 absorption [15,16]. Also, in SF_6 L emission using S $2p$ resonant excitation one observes emission emerging at 151–152 eV when exciting to the $2p^5\,4e_g^*$ state around 196 eV [17], suggesting dissociation of the excited neutral molecule. Note that, in our present work, the relaxation of the deep $1s$ hole involves multiple steps with charged or multiply charged intermediate states, whereas in the mentioned studies, the relaxation of shallow $2p$ holes occurs through a single radiative step, leading directly to neutral final configurations.

To model the (stepwise) decay of the initial $1s$ hole in sulfur, advanced energy-level and transition-rate calculations were performed. This relaxation of a well-localized core hole can be formally described by an atomic cascade that connects ions of various charge states via different radiative and autoionization processes [18]. Particularly for atoms (and molecules) with holes in the inner shell, the multiconfiguration Dirac-Hartree-Fock method has proven to be versatile in dealing with the interplay of different relaxation processes in the course of stabilization of the atoms and ions [19–21]. To model such cascades, we used the JAC toolbox, the Jena Atomic Calculator [22], which has recently been extended to handle and analyze sizable ionization pathways. The focus was placed on the decay of the $1s2s^22p^63s^23p^5$ and $1s2s^22p^63s^23p^4$ (initial) configurations and how the (relative) population of associated fine-structure levels propagates through the cascade. A series of cascade calculations implemented in the JAC toolbox were performed to examine the population of S $2p^5$ hole states formed during the second or third step of the relaxation decay cascade. This cascade follows the first step of *KLL* Auger decay, which is dominant over other decay channels. S $2p^5$ hole states are also formed after the *KLM* Auger and K_α decay of the S $1s$ core hole, but with a significantly lower cross section [23]. The numerical results together with the experimental measurements are discussed below.

The calculated energy levels clearly confirm that the photon emission at 151–152 eV results from a $3s \rightarrow 2p$ transition, although the charge state of the sulfur ions was initially much less apparent. In fact, all $2p^53s^23p^m$ ($m = 4, \ldots, 1$) hole configurations of S^{q+} support $3s \rightarrow 2p$ photon emission with energies nearby, but generally higher than observed in the measurements. The rapid autoionization of a $1s^{-1}$ core hole typically results in an extensive fine structure of the S $2p$ core-hole states, along with many other dipole transitions that are allowed but not observed.

The calculations provide photon emission energies as well as radiative and nonradiative rates for the transitions

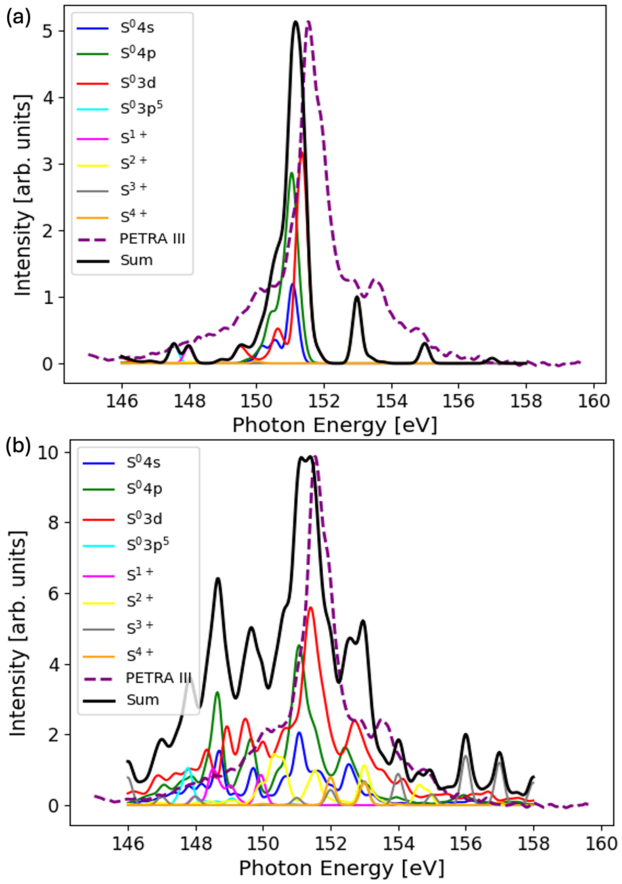

FIG. 3. (a) Calculated sulfur L emission involving the 10% lowest of all neutral and charged S $2p$ hole states, compared to the experimental emission spectrum excited at 2487 eV (dotted line). (b) Corresponding calculated spectrum accounting for all of the possible initial states. Plotted intensity is proportional to line strength multiplied by fluorescence yield. The spectra are convoluted with a 0.3 eV FWHM Gaussian function.

from all states of the neutral electron configurations $2p^53s^23p^5$, $2p^53s^23p^43d$, $2p^53s^23p^44s$, $2p^53s^23p^44p$, and the $n=1$ to $n=4$ charged configurations $2p^53s^23p^{5-n}$. Since the Auger rate may vary significantly for different transitions, the line strengths need to be weighted by the calculated fluorescence yield. Spectra based on the calculations were synthesized by summing the Gaussian broadened line intensities on a photon-energy scale and are presented as graphs in Fig. 3. Figure 3(a) shows the sulfur L emission from the 10% lowest $2p$ hole states for all charge states, from neutral to 4+ since the preceding S $1s$ deexcitation process populates preferentially energetically lower states with a S $2p$ hole. In Fig. 3(b), the corresponding transitions for all states are shown. The experimental L emission from SF_6 excited on the S $1s \rightarrow 6t_{1u}$ resonance at 2487 eV is also displayed as reference. In the Supplemental Material [14], plots also for 75%, 50%, 25%, and 5% fractions of states are shown.

The calculations show in particular that all charged configurations with a S $2p$ hole give rise to spectra that extend over several eV and have only partial overlap with the observed spectrum (see Fig. 1 in the Supplemental Material [14]). Also, considering the significant chemical shift, caused by the strong electronegativity of the fluorine atoms, the observed photon emission lines are unlikely to originate from positively charged molecular fragments.

When all the initial $2p$ hole states are included, the calculated spectrum is clearly not compatible with the overall shape of the experimental spectrum. Still, the dominant components arise from the neutral species with $3d$, $4s$, and $4p$ spectator occupancy, whereas the charged species contribute negligible intensity. In Fig. 3(a), where only the 10% lowest states contribute, quite good agreement with experiment is seen, knowing the expected accuracy of the calculated transition energies of about 1 eV. Here too, the contribution of the neutral species of $3d$, $4s$, and $4p$ almost completely forms the resulting spectrum.

The finding that the spectral feature at 151–152 eV is primarily due to photon emission from neutral atoms is indeed prominent given the electronegative character of fluorine and that photon emission must occur independently of the initial charge state and level population of sulfur after the photon impact. Nevertheless, the presence of neutral sulfur can be understood by the charge concentration of the $3p$-$2p$ electron pairs, that form the chemical bonds of the SF_6 molecule, due to screening of the inner-shell holes in sulfur by valence electrons; these inner-shell holes in the S $1s$, S $2s$, and S $2p$ core orbitals lead to a compression of electron density around the sulfur atom. Therefore, when intermediate $(SF_6)^{q+}$ ions undergo dissociation, F^+ ions are ejected, leaving behind sulfur or sulfur-containing molecular fragments with reduced or even neutral charge. Notably, mass-spectroscopy measurements performed around the ionization threshold of S $1s$ show a significant dominance of F^+ ions, accounting for ~60% of the total ion yield [24], while atomic S^{n+} cations ($n \leq 4$) account for only ~21%, with the contribution of S^+ and S^{2+} ions being ~14% and ~6%, respectively (see results from COLTRIMS measurements in the Supplemental Material [14,25–30]).

In the atomic calculations, this charge concentration can still be modeled by a S $2p^53s^23p^m$ ($m \leq 4$) configuration despite the prior autoionization. To gain deeper insight into the redistribution of valence-electron density due to screening effects of S $1s$ and S $2p$ core-hole states, we conducted a Mulliken population analysis [31,32] specifically targeting the $4t_{1u}$ bonding orbitals. For an illustration of the molecular orbital structure of SF_6, see, e.g., Ref. [33]. These orbitals are the highest-lying bonding molecular orbitals and arise from the linear combination of the $3p$ atomic orbitals of S and the $2p$ atomic orbitals of F:

$$4t_{1u} = c_0 3p_S \pm \Sigma_i c_i 2p_{i,F}, \quad (1)$$

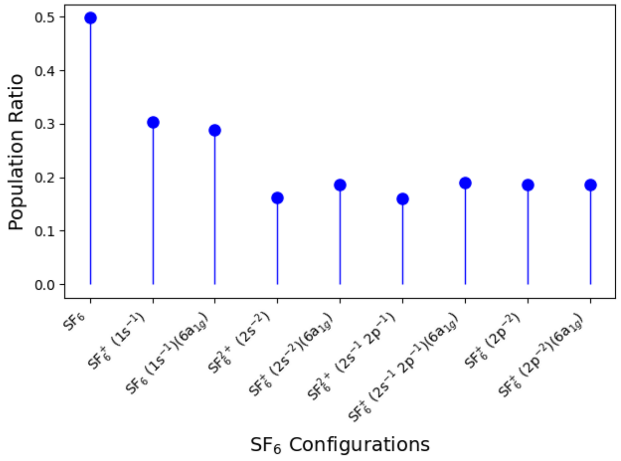

FIG. 4. F $2p$/S $3p$ ratio of Mulliken populations for the $4t_{1u}$ molecular orbitals in SF_6.

where the squares of the c_i combination coefficients define the Mulliken population associated with each combined orbital. To investigate whether orbital localization could be a reason for the unexpected electron retention of the sulfur atom in the dissociation process a Mulliken population analysis was performed for SF_6 in the ground state and in a series of different core-hole states that arise during the decay of the $1s$ core-hole state.

In Fig. 4, we present the F $2p$/S $3p$ ratio of Mulliken populations for the $4t_{1u}$ molecular orbitals. This ratio decreases from 0.5 in the ground state to 0.3 in the S $1s^{-1}$ states and to 0.2 in the S $2p^{-2}$ core-hole states, indicating the localization of bonding electrons on sulfur as specific core-hole configurations emerge on the sulfur atom. Notably, the ratio is one of the lowest for configurations involving S $2p^{-2}$ double core holes, which are prevalent in the dominant *KLL* Auger decay. Because of the localization of the bonding electrons on the sulfur atom during electronic relaxation, we find a rationale for the observation that neutral sulfur makes the dominant contribution to the L-emission spectrum. The neutral sulfur observed in the experiment is therefore explained by delocalization of binding valence electrons toward sulfur from the surrounding fluorine atoms in the course of the sulfur core-hole cascade decay.

In this work, the sulfur L emission from SF_6 gas excited at different photon energies below, at, and above the S $1s \rightarrow 6t_{1u}$ resonance was studied. The resulting spectra show a composite structure with varying intensity across the resonance, and slight variations in the weights of individual components. The spectral structure appears at 151–152 eV, exactly where a group of very narrow atomic lines was observed in an early high-resolution study using 10 keV electron-beam excitation. This result shows that dissociation of SF_6 leads to sulfur L x-ray emission from predominantly neutral species after S $1s$ excitation or ionization, despite the dominant autoionization of a S $1s$ initial hole, which involves one or more Auger electrons. During dissociation, delocalization of the electron density neutralizes the sulfur atom before L emission, as the (missing) screening charge can still be attracted from the surrounding fluorine atoms. Furthermore, the relative weight of the molecular lines was found to increase above the S $1s$ resonance, indicating a higher dissociation probability upon resonant excitation. Importantly, the clear observation of L emission above the S $1s$ threshold underscores that MUST UFD is a general phenomenon, independent of photon energy, as long as it is sufficient to create a deep core hole. This experiment successfully demonstrates the efficacy of x-ray emission techniques in probing ultrafast dynamics during cascade decays, which typically produce multiply charged intermediates following deep-core electron emission. In the future, it would be essential to explore the mechanisms of dissociation and charge redistribution during cascade decays, as well as to investigate the timescales of these processes. Utilizing pump-probe techniques at x-ray free-electron laser facilities could provide valuable insights into the ultrafast dynamics involved for a deeper understanding of the underlying phenomena.

Acknowledgments—We acknowledge DESY (Hamburg, Germany), a member of the Helmholtz Association HGF, for the provision of experimental facilities. Parts of this research were carried out at PETRA III and we would like to thank M. Hoesch and his team for assistance in using beamline P04. Beamtime was allocated for proposal I-20211270 EC. O. T. acknowledges funding by the French Agence Nationale de la Recherche (ANR) through the MUSTACHE project (ANR-18-CE30-0015). F. T. acknowledges funding by the Deutsche Forschungsgemeinschaft (DFG, German Research Foundation) – Project 509471550, Emmy Noether Programme. N. V. and T. M. acknowledge funding from the European Union's Horizon 2020 research and innovation program under the Marie Skłodowska-Curie Grant Agreement No. 860553. M. H. acknowledges funding by the German Federal Ministry of Education and Research under Grant No. 13K22XXB DYLIXUT. J.-E. R. acknowledges support from the Swedish Research Council (VR Contract No. 2021-04017). J. N. acknowledges the Carl Trygger Foundation for financial support.

[1] M. O. Krause, J. Phys. Chem. Ref. Data **8**, 307 (1979).
[2] O. Travnikova, T. Marchenko, G. Goldsztejn, K. Jänkälä, N. Sisourat, S. Carniato, R. Guillemin, L. Journel, D. Céolin, R. Püttner, H. Iwayama, E. Shigemasa, M. N. Piancastelli, and M. Simon, Phys. Rev. Lett. **116**, 213001 (2016).
[3] A. Pietzsch, Y.-P. Sun, F. Hennies, Z. Rinkevicius, H. O. Karlsson, T. Schmitt, V. N. Strocov, J. Andersson, B. Kennedy, J. Schlappa, A. Föhlisch, J.-E. Rubensson, and F. Gel'mukhanov, Phys. Rev. Lett. **106**, 153004 (2011).

[4] T. Marchenko, S. Carniato, L. Journel, R. Guillemin, E. Kawerk, M. Žitnik, M. Kavčič, K. Bučar, R. Bohinc, M. Petric, V. Vaz da Cruz, F. Gel'mukhanov, and M. Simon, Phys. Rev. X **5**, 031021 (2015).

[5] O. Travnikova, N. Sisourat, T. Marchenko, G. Goldsztejn, R. Guillemin, L. Journel, D. Céolin, I. Ismail, A. F. Lago, R. Püttner, M. N. Piancastelli, and M. Simon, Phys. Rev. Lett. **118**, 213001 (2017).

[6] E. Ertan, V. Savchenko, N. Ignatova, V. Vaz da Cruz, R. C. Couto, S. Eckert, M. Fondell, M. Dantz, B. Kennedy, T. Schmitt, A. Pietzsch, A. Föhlisch, F. Gel'mukhanov, M. Odelius, and V. Kimberg, Phys. Chem. Chem. Phys. **20**, 14384 (2018).

[7] K. Yamazoe, J. Miyawaki, H. Niwa, A. Nilsson, and Y. Harada, J. Chem. Phys. **150**, 204201 (2019).

[8] H. Ågren, J. Nordgren, L. Selander, C. Nordling, and K. Siegbahn, Phys. Scr. **18**, 499 (1978).

[9] J. Nordgren, H. Ågren, C. Nordling, and K. Siegbahn, Phys. Scr. **19**, 5 (1979).

[10] C. Nicolas and C. Miron, J. Electron Spectrosc. Relat. Phenom. **185**, 267 (2012).

[11] J. Viefhaus, F. Scholz, S. Deinert, L. Glaser, M. Ilchen, J. Seltmann, P. Walter, and F. Siewert, Nucl. Instrum. Methods Phys. Res., Sect. A **710**, 151 (2013).

[12] J. Nordgren, G. Bray, S. Cramm, R. Nyholm, J.-E. Rubensson, and N. Wassdahl, Rev. Sci. Instrum. **60**, 1690 (1989).

[13] www.javu.se, Carbon membranes for x-ray spectroscopy (2024).

[14] See Supplemental Material at http://link.aps.org/supplemental/10.1103/PhysRevLett.134.063003 for supplementary information on theoretical calculations, Mulliken population calculations, further experimental results, and COLTRIMS measurements on SF_6.

[15] M. Magnuson, J. Guo, C. Såthe, J.-E. Rubensson, J. Nordgren, P. Glans, L. Yang, P. Sałek, and H. Ågren, Phys. Rev. A **59**, 4281 (1999).

[16] R. F. Fink, A. Eschner, M. Magnuson, O. Björneholm, I. Hjelte, C. Miron, M. Bassler, S. Svensson, M. N. Piancastelli, and S. L. Sorensen, J. Phys. B **39**, L269 (2006).

[17] N. Kosugi, J. Electron Spectrosc. Relat. Phenom. **137–140**, 335 (2004).

[18] S. Fritzsche, P. Palmeri, and S. Schippers, Symmetry **13**, 520 (2021).

[19] P. S. Bagus and H. F. Schaefer, III, J. Chem. Phys. **55**, 1474 (1971).

[20] A. Szabo and N. S. Ostlund, *Modern Quantum Chemistry: Introduction to Advanced Electronic Structure Theory* (Dover Publications Inc., New York, 1982).

[21] T. Saue, R. Bast, A. S. Pereira Gomes, H. J. A. Jensen, L. Visscher, I. A. Aucar, R. Di Remigio, K. G. Dyall, E. Eliav, E. Fasshauer *et al.*, J. Chem. Phys. **152**, 204104 (2020).

[22] S. Fritzsche, Comput. Phys. Commun. **240**, 1 (2019).

[23] F. von Busch, U. Kuetgens, J. Doppelfeld, and S. Fritzsche, Phys. Rev. A **59**, 2030 (1999).

[24] A. H. A. Gomes, R. R. Oliveira, A. B. Rocha, W. Wolff, K. F. Alcantara, G. M. Sigaud, and A. C. F. Santos, Int. J. Mass Spectrom. **388**, 9 (2015).

[25] R. Dörner, V. Mergel, O. Jagutzki, L. Spielberger, J. Ullrich, R. Moshammer, and H. Schmidt-Böcking, Phys. Rep. **330**, 95 (2000).

[26] J. Ullrich, R. Moshammer, A. Dorn, R. Dörner, L. Ph. H. Schmidt, and H. Schmidt-Böcking, Rep. Prog. Phys. **66**, 1463 (2003).

[27] T. Jahnke, Th. Weber, T. Osipov, A. L. Landers, O. Jagutzki, L. Ph. H. Schmidt, C. L. Cocke, M. H. Prior, H. Schmidt-Böcking, and R. Dörner, J. Electron Spectrosc. Relat. Phenom. **141**, 229 (2004).

[28] O. D. McGinnis, Photoelectron Diffraction Imaging of SF_6, Bachelor's thesis, Goethe-Universität Frankfurt am Main, 2021.

[29] O. Jagutzki, V. Mergel, K. Ullmann-Pfleger, L. Spielberger, U. Spillmann, R. Dörner, and H. Schmidt-Böcking, Nucl. Instrum. Methods Phys. Res., Sect. A **477**, 244 (2002).

[30] O. Jagutzki, J. S. Lapington, L. B. C. Worth, U. Spillman, V. Mergel, and H. Schmidt-Böcking, Nucl. Instrum. Methods Phys. Res., Sect. A **477**, 256 (2002).

[31] R. S. Mulliken, J. Chem. Phys. **23**, 1833 (1955).

[32] R. S. Mulliken, Science **157**, 13 (1967).

[33] Charlesy, Molecular orbital diagram of SF_6, Wikimedia Commons, the free media repository (2018), https://commons.wikimedia.org/wiki/File:MO_diagram_sulfur_hexafluoride.png.